Repetitive Load Test on a Composite Precast-Decked Bridge Model

ROBERTO A. OSEGUEDA AND JAMES S. NOEL

The results of a repetitive load test conducted on a laboratory model to study the deterioration of connections designed to develop composite behavior in precast-decked steel bridges are presented. Two million sinusoidal load cycles at a frequency of 3.5 Hz at levels exceeding those of an equivalent HS 20-44 AASHTO truck were applied to a ⅓-scale laboratory model of a composite, precast-decked, simple-span bridge. Loads, deflections, strains, and relative deck-beam displacements were continuously monitored and recorded at several time windows. The dynamic measurements were approximated to the steady state response by curve-fitting 3.5 Hz sinusoidal wave functions from which the amplitudes of measurements were obtained. The amplitudes of deflections, composite moments of inertia of two sections, and relative deck displacements were analyzed and graphed versus the cycle number. A statistical test was conducted to establish the significance of the test results. The flexibility of the structure increased by less than 7 percent. The flexural properties of the two instrumented sections remained constant. The amplitude of relative deck-beam displacements remained negligible throughout the test. No evidence was found of any deterioration of the deck-beam interface connections.

The use of full-depth precast concrete panels for the replacement of bridge decks is expected to grow as deterioration problems on decks continue. Two major advantages offered by the precast replacement method over other methods are (a) on-site reconstruction is fast, and (b) traffic on the bridge during the reconstruction is allowed. These advantages were recognized as early as 1973 (*1*). Since then, several bridges have been replaced using precast concrete panels (*2–6*).

In the precast replacement method, the panels are connected to each other and to supporting longitudinal steel beams to form a monolithic unit. Connections between adjacent panels are usually accomplished with grouted keyways (*1,2,4,6*). Uniform bearing and vertical alignment of the panels of steel beams are obtained by the placement of a thick mortar before setting the panels (*1*), by use of bearing pads with the grout placed after setting the panels (*4*), or by use of bolt-leveling supports adjusted while the mortar bed is being placed (*3*).

All precast decks reconstructed to date can be classified according to their design as noncomposite or composite. In noncomposite designs, the applied loads are assumed to be resisted by the beams only; whereas in composite designs the loads are assumed to be resisted by the precast slab and beams combined. A difference between the construction of the two designs is that noncomposite bridges use tie anchors or bolts to connect the panels to the beams and composite bridges use steel-headed studs housed in blockout holes filled with grout to ensure the transfer of horizontal shear between the deck and the beams by mechanical means.

Both designs typically include an adhesive layer of epoxy or polymer grout between the deck and the beams. The adhesive action of this material physically bonds the precast deck to the beams and may have sufficient strength to cause composite behavior at normal service load levels (*2*). Therefore, the use of shear connectors only ensures the composite interaction by mechanical means in the event of an adhesive bond failure.

The question that arises is what should be the fatigue design criteria for shear connectors used in this type of construction. There are two factors that should be considered. First, the AASHTO bridge design specifications (*7*) only allow for a composite design if mechanical shear connectors are provided (see Section 10.38.2). Second, AASHTO fatigue design equations for shear connectors (Section 10.38.5.1.1) were developed for connectors embedded in normal concrete (*8–10*) and not in other embedment materials.

The objectives are to report the results of a repetitive load test conducted on a scaled model of a precast-decked, simple-span bridge; to describe the performance of the model during a repetitive load test; and to discuss the adequacy of existing fatigue design criteria for shear connectors embedded in epoxy materials.

DESCRIPTION OF THE MODEL

The laboratory structure was a ⅓-scale model of a typical middle portion of a 60-ft steel stringer bridge decked with precast concrete panels. A layout of the model is shown in Figure 1. The details of the model beams are shown in Figure 2. The I-beams of the model were W 12 × 19 steel sections modified to scale W 36 × 150 section beams with cover plates at the top and bottom flanges. The modifications were necessary to scale the moments of inertia of the prototype beams by a factor of 1/81 and consisted of the cover plates and reductions of the flange width at the ends as shown in Figures 2a and 2d. The model beams also included pairs of ¼-in. steel studs welded at a 6-in. spacing. The laboratory model was designed using laws of similitude (*11*) to have the same live load stresses as the 60-ft prototype bridge. Concentrated loads and shear forces on the prototype scale by a factor of 1/9 to the model, and bending moments scale by a factor of 1/27. Modeling of dead weight was not considered because only live load stresses were of interest for this study.

The deck of the bridge model was made with 10 precast panels interconnected to each other and connected to the steel

R. A. Osegueda, Department of Civil Engineering, University of Texas at El Paso, El Paso, Tex. 79968-0516. J. S. Noel, Department of Civil Engineering, Texas A&M University, College Station, Tex. 77843.

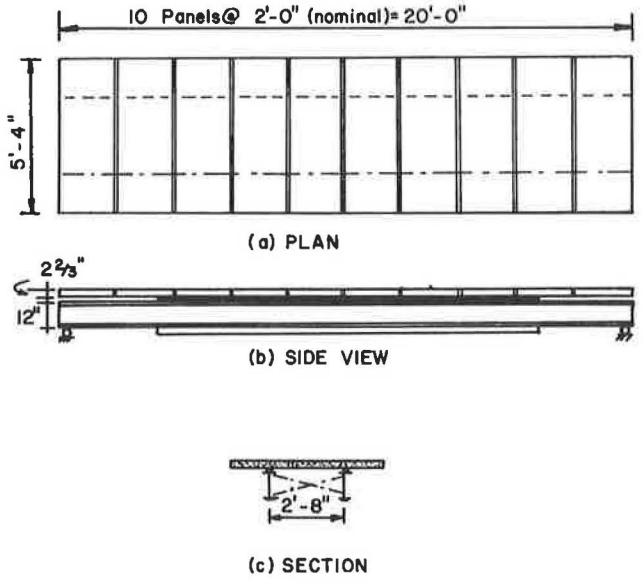

FIGURE 1 Layout of laboratory model: (a) plan view, (b) side view, and (c) typical section.

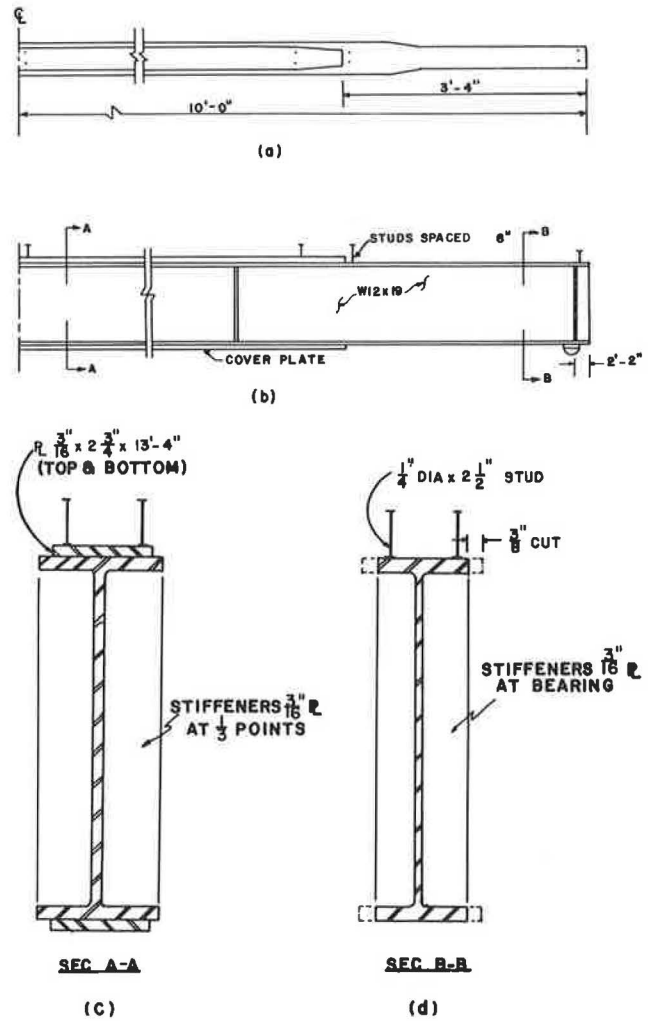

FIGURE 2 Details of model beams: (a) half-plan view, (b) half-elevation, (c) typical cover-plated section, and (d) typical end section.

beams. Each panel had nominal dimensions of 24 in. long and 64 in. wide. A typical panel is shown in Figure 3. Block-out holes were included to house shear connectors. Grooves were molded at the transverse sides so that shear keyways were formed between adjacent panels (Figure 3b). The block-out holes, the shear keyways, and the deck-beam interface gaps were grouted using an epoxy mortar obtained by mixing dry silica sand with epoxy binder THD–B–102 (similar to type VIII ASTM C–881) at a three-to-one proportion by weight. Tests conducted on epoxy mortar cylindrical samples at 7 days yielded a minimum compressive strength of 12,000 psi, split tensile strength of 1,500 psi, and an initial tangent modulus of 1.20×10^6 psi. The concrete mix for the panels consisted of typical volume proportions of scaled aggregates and cement. Results of concrete cylinder tests conducted at 28 days exhibited compressive strength values in excess of 6,000 psi. Welded wire fabric was used to simulate typical reinforcement. Complete details of the design and construction procedures of the model are described by Osegueda and Noel (*11*).

LOADING HISTORY OF THE MODEL

Before the repetitive load test, the model experienced two load test programs. In the first program (*11*), the model was statically tested up to bending stress levels equivalent to 150

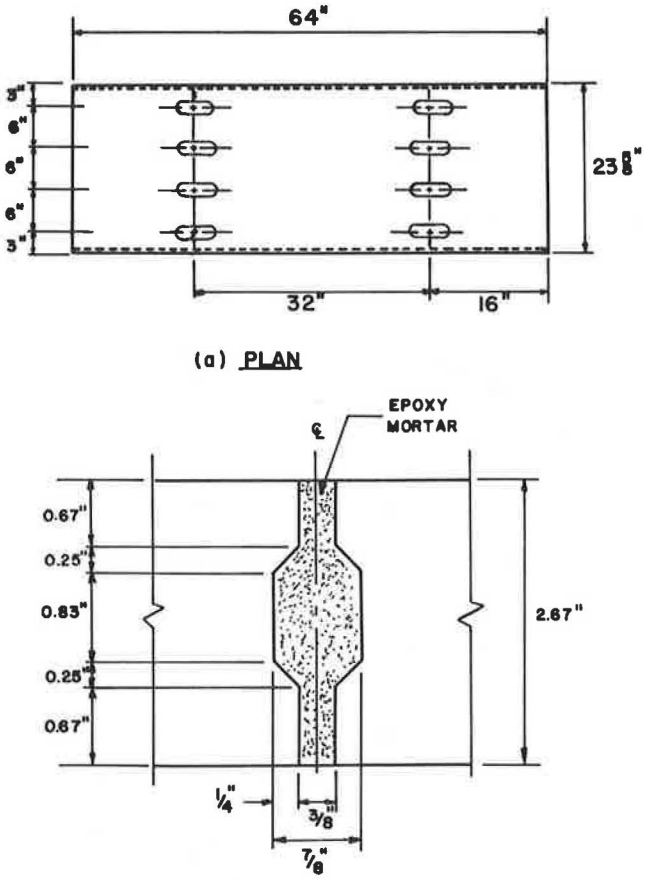

FIGURE 3 (a) Typical precast panels and (b) shear keyway.

percent of the stress levels caused by an HS 20-44 AASHTO truck. The load was applied at the third points of the model and the elastic range of the steel beams was never exceeded. The second test program consisted of evaluating the performance of the precast deck when subjected to negative moments (*12*). The model was anchored at the supports and was loaded with equal upward concentrated forces applied at the midspan of both beams. This loading sequence caused transverse cracking at the keyways and at the concrete mass in the vicinity of the midspan. This second test program led to the conclusion that the method is not adequate for redecking in negative-moment regions. However, no cracking or debonding was observed in the deck-beam interfaces. Thus, when the repetitive load test program started, the deck was severely cracked. However, because the cracks were formed by the application of negative moments, they were observed to close when the bridge model was subjected to positive moments.

INSTRUMENTATION AND TEST PROCEDURE

The set-up of the model for the repetitive load test is shown in Figure 4. Two equal cycling loads were applied to each beam while the centroid of the loads was located 36 in. from the midspan towards a high-shear side. The loading and instrumentation systems consisted of two closed-loop, 55-kip hydraulic actuators and a computerized data acquisition and control system. A spreader beam attached to the bottom of each actuator was used to equally distribute the actuator load to two points per beam.

The instrumentation installed in the model consisted of strain gauges and displacement transducers. Figure 5 shows the location of the measuring points. Strain gauges were used to measure flexural strains at two different cross sections of the north beam of the model (Figure 5c). Displacement transducers were used to measure deflections at the inside quarter-points of the north beam (Figure 5b) and relative horizontal displacements between the precast deck and the beams at Locations 1 through 5 (Figure 5a). The instrumentation was complemented with the load cell and displacement transducer of each actuator. A total of 20 channels of information was used.

Two million cycles of sinusoidal loads were applied to the model at a frequency of 3.5 Hz. Each actuator was controlled to provide loading cycles oscillating between 1,700 and 9,900 lb in compression and to give a total load range of 8,200 lb per actuator. The test was executed continuously for about 8 days and was totally computerized. The computer was programmed to count cycles and to trigger the data acquisition equipment hundreds of times during the test. Each time the data acquisition system triggered, it sampled each of the 20 channels for a lapse time of 0.75 sec at a rate of 100 Hz per channel (one point every 0.01 sec). The data points were then stored along with their corresponding cycle number. When the cycle count was 2 million, the test stopped automatically.

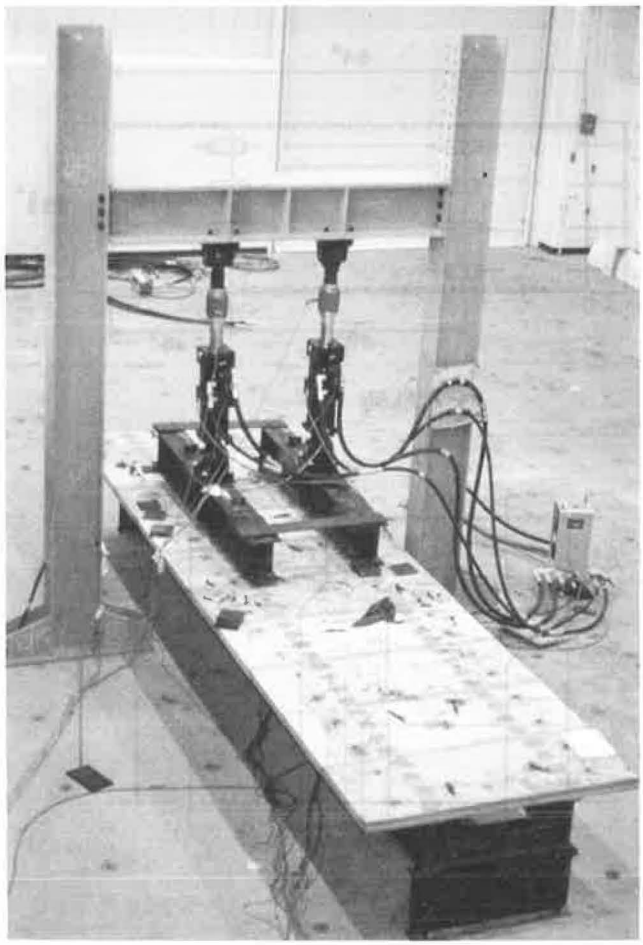

FIGURE 4 View of test setup.

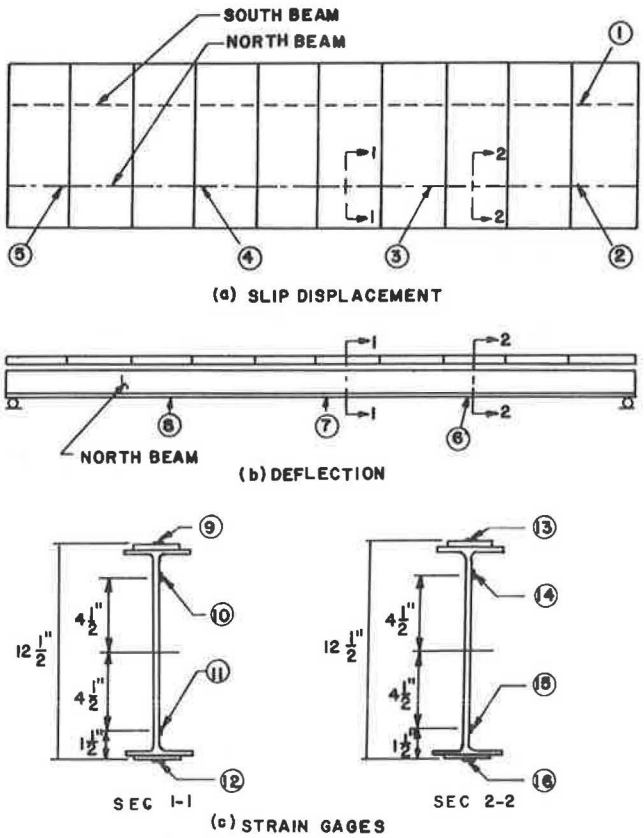

FIGURE 5 Instrumented locations: (a) deck-beam horizontal displacements, (b) deflections, and (c) strains.

EQUIVALENT LOAD LEVELS

In this section, the applied loads on the model are extrapolated to a 60-ft prototype bridge, and the extrapolated load levels of the prototype are compared to those produced by a single HS 20–44 AASHTO truck. The maximum and minimum shear and moment diagrams of the beams are shown in Figure 6. In these diagrams, dynamic amplifications have been conservatively neglected. The maximum end shear on the beams was 6.5 kips and the maximum shear range was 5.4 kips. The maximum moment and moment range were 32.8 and 27.2 kip-ft, respectively, under the point load near the midspan. The maximum total load on the model was 18.4 kips and the load range was 16.4 kips. Because the model is at a scale of 1/3, shears and point loads extrapolate to the prototype with a factor of 9, and bending moments extrapolate with a factor of 27. Table 1 presents a comparison of the extrapolated load levels and the levels caused by an HS 20-44 AASHTO truck on the 60-ft prototype. The prototype HS 20-44 load levels were computed using procedures of the AASHTO bridge specifications (*7*). The loads applied to the model exceeded the levels of an equivalent HS 20-44 AASHTO truck. More important, the shear range levels, which may cause fatigue in the interface connections, were 128 percent of those expected from an HS 20-44 truck.

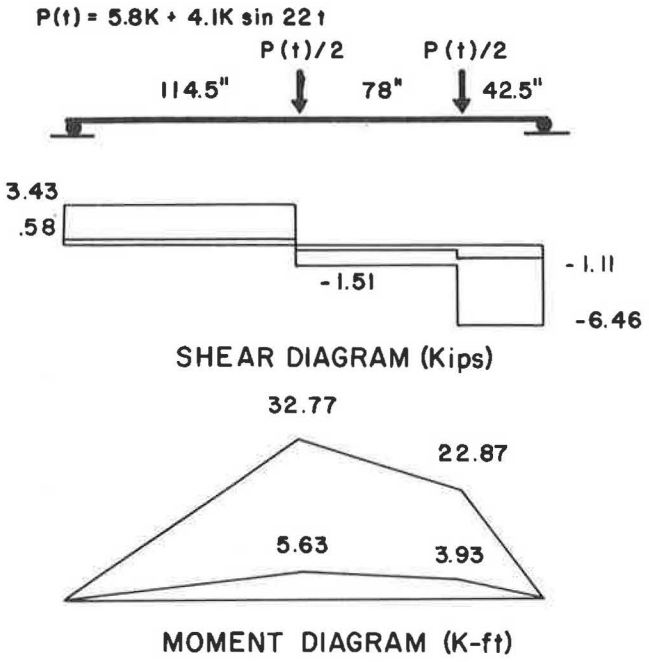

FIGURE 6 Maximum and minimum shear and bending moment diagrams.

The maximum shear range in the model translates to a maximum horizontal shear range of 1.35 kips per connector or a shear stress range of 28 ksi if the adhesive action of the deck-beam interface material is totally neglected. In contrast, Section 10.38.5.1.1 of the AASHTO bridge specifications (*7*) only allows 10 ksi of shear stress range on the connectors if a design for 2 million cycles is considered.

TEST RESULTS

During the test, data from each channel were collected and recorded for 826 different time windows, each window lasting 0.75 sec. The results typify measured raw data for loads, strains, deflections, and relative deck-beam displacements. The signals measured at Cycle 10 are illustrated.

Figure 7 shows a typical measurement of the applied load signal as recorded from the load cells of one of the actuators. The load was oscillating between −1,700 and −9,900 lb (the negative sign indicates compression). Figure 8 shows the deflection measured at the midspan of the north beam. Similar deflection signals were measured at the other two quarter-points. Figures 9 and 10 show strain measurements made at

TABLE 1 EQUIVALENT PROTOTYPE LOAD LEVELS

	APPLIED IN MODEL	EQUIVALENT TO PROTOTYPE	PROTOTYPE HS 20-44 LEVEL	PERCENT LEVEL WRT HS 20-44
Total Live Load (kip)	19.8	178	91	196%
Total Live Load Range (kip)	16.4	148	91	162%
Max. End Shear (kip)	6.5	58.5	38	154%
Max. End Shear Range (kip)	5.4	48.6	38	128%
Max. Moment (k-ft)	32.7	885	727	122%
Max. Moment Range	27.2	734.4	727	101%

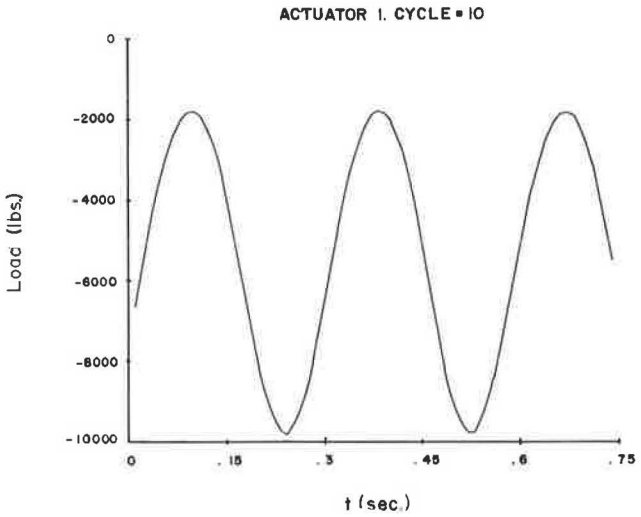

FIGURE 7 Typical load signal.

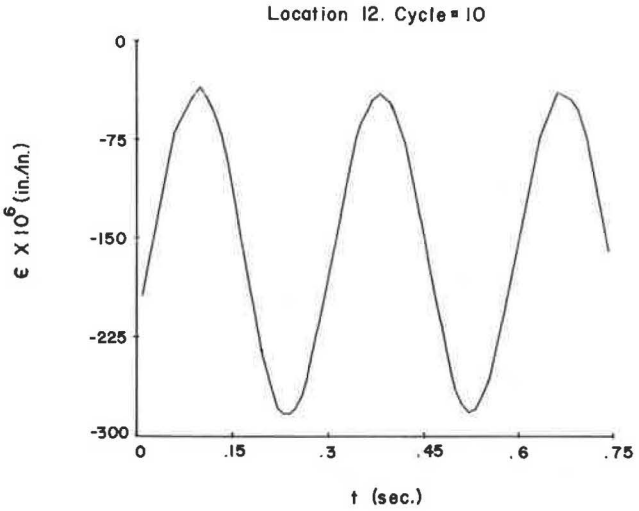

FIGURE 10 Typical strain signals at Section 1: bottom flange.

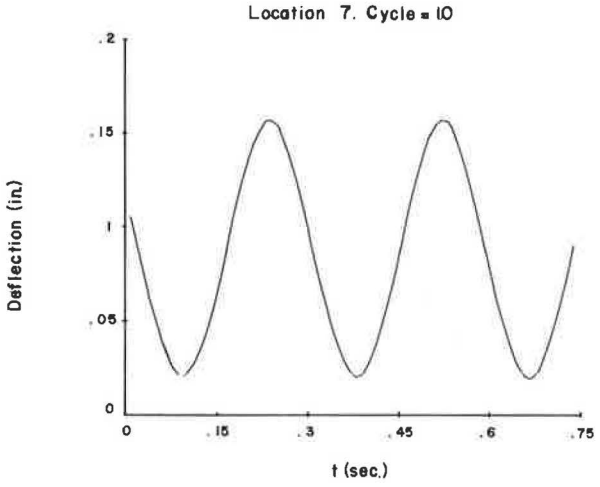

FIGURE 8 Typical deflection signal.

the top and bottom flanges, respectively, of Section 1 of the north beam. The strain measurements at the top flange (Figure 9) were contaminated with electronic noise. This problem was only typical for those measurements with small amplitudes. Similar signals were recorded from the other strain gauges bonded to Sections 1 and 2.

The measured relative deck-beam horizontal displacements were severely contaminated with noise because these displacements were of the order of 0.001 in. The major function of these measurements was to detect failure or debonding of the interface connection. Failure of the interface should have reflected dramatic increases in the relative deck-beam displacements. Figure 11 shows the relative displacement measured at Location 1 at the high-shear end of the south beam. The solid line represents a curve-fitted sinusoidal curve with a frequency of 3.5 Hz.

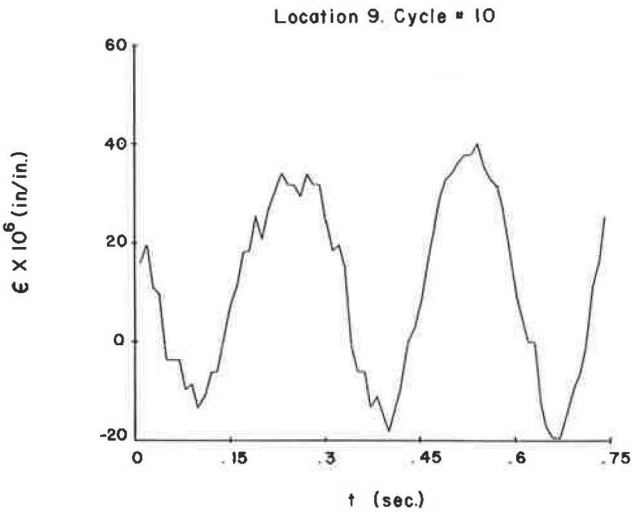

FIGURE 9 Typical strain signals at Section 1: top flange.

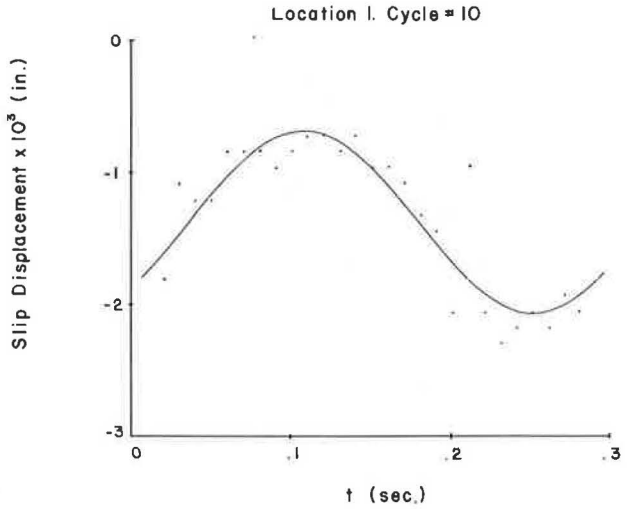

FIGURE 11 Typical relative deck-beam horizontal displacement.

ANALYSIS OF EXPERIMENTAL MEASUREMENTS

To correct the signals from noise, the measurement of load, strains, deflections, and relative displacements were curve-fitted using a sine wave function. The measured signals were assumed to have a predominant oscillating frequency of 3.5 Hz. The data were approximated to the steady state response by functions all of which had the form

$$g(t) = A + B \sin \omega t + C \cos \omega t \tag{1}$$

where A, B, and C are regression constants and ω is the loading frequency of 7.0π rad/sec.

By minimizing the square of the errors between the functions $g(t)$ and the n measured points $f(t_i)$, the regression constants were determined by the equation

$$\begin{pmatrix} A \\ B \\ C \end{pmatrix} = \begin{pmatrix} n & \Sigma \sin \omega t_i & \Sigma \cos \omega t_i \\ \Sigma \sin \omega t_i & \Sigma \sin^2 \omega t_i & \Sigma \sin \omega t_i \cos \omega t_i \\ \Sigma \cos \omega t_i & \Sigma \sin \omega t_i \cos \omega t_i & \Sigma \cos^2 \omega t_i \end{pmatrix}^{-1} \cdot \begin{pmatrix} \Sigma f(t_i) \\ \Sigma f(t_i) \sin \omega t_i \\ \Sigma f(t_i) \cos \omega t_i \end{pmatrix} \tag{2}$$

Subsequently, Equation 1 was written as

$$g(t) = A + \frac{\alpha}{2} \sin (\omega t - \psi_0) \tag{3}$$

where $\alpha = 2(B^2 + C^2)^{1/2}$ and $\psi_0 = \tan^{-1}(B/C)$.

In Equation 3, α is the total amplitude of the approximated function and ψ_0 is the phase angle.

This curve-fitting technique was performed to extract the amplitudes of loads, deflections, relative displacements, and strains for each recorded window of data. The extracted amplitudes were then normalized with respect to the load amplitude.

Deflections

The amplitude of deflections extracted for locations 6 through 8 of the north beam (see Figure 5) were normalized by obtaining the corresponding flexibility. The deflection amplitude at a given window was divided by the amplitude of load of the same window. The flexibility values were then plotted against the cycle number. These graphs are shown in Figures 12 through 14. The dynamic flexibility was slightly increasing as the number of load cycles increased.

Flexural Strains

The amplitude of the flexural strains recorded at Locations 9 through 12 and 13 through 16 were used to obtain the dynamical moments of inertia of Sections 1 and 2, respectively, as

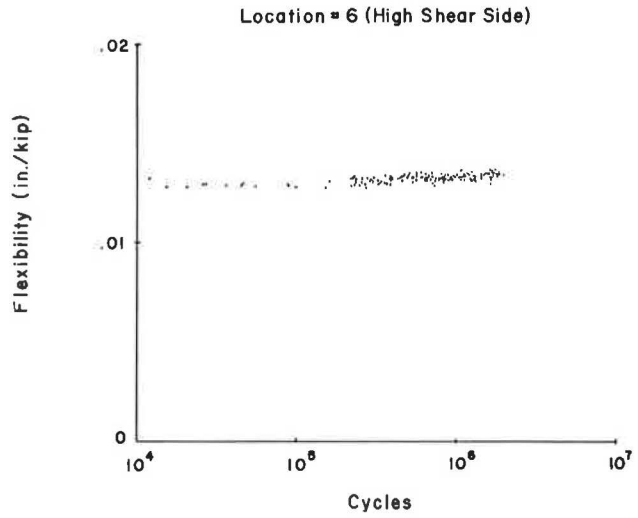

FIGURE 12 Flexibility at quarter points of north beam: high-shear side.

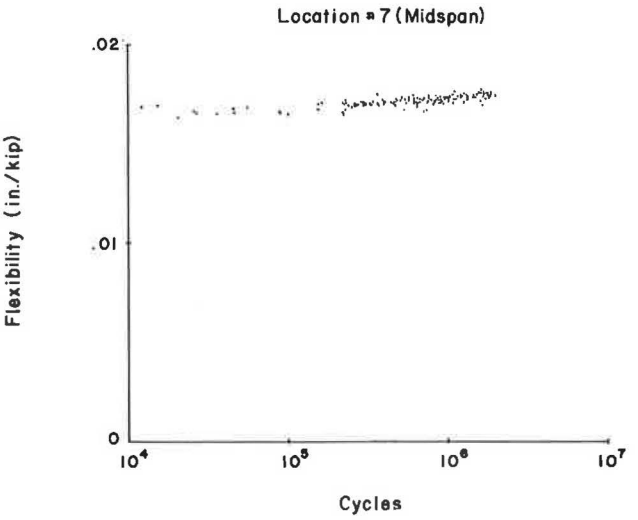

FIGURE 13 Flexibility at quarter points of north beam: midspan.

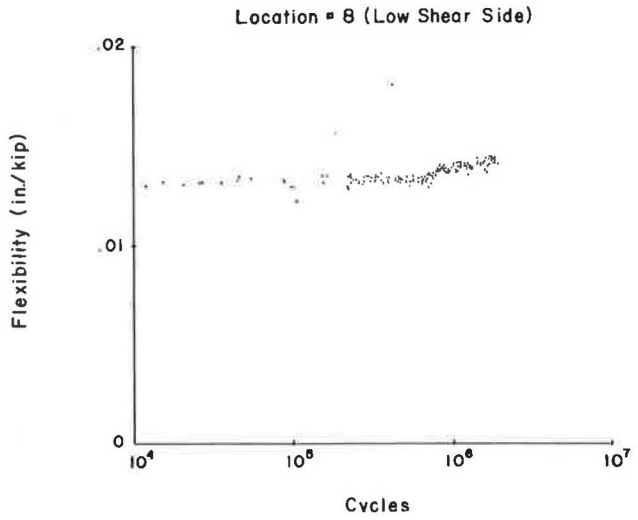

FIGURE 14 Flexibility at quarter points of north beam: low-shear side.

functions of the number of cycles. It is observed from Figure 15 that a straight-line fit of strain amplitudes corresponds to an equation of the form

$$\varepsilon(y) = \varepsilon_b + \phi y \tag{4}$$

where

ε_b = strain amplitude at the bottom fibers,
ϕ = amplitude of curvature, and
y = vertical distance from the bottom fibers.

If the dynamic moment is known and linear elastic behavior is assumed, then the dynamic moment of inertia of the composite section can be determined from the equation

$$I = \frac{mP}{E\phi} \tag{5}$$

where

P = load amplitude,
m = moment at the corresponding section caused by a unit load,
E = modulus of elasticity of steel (29,000 ksi), and
ϕ = amplitude of curvature.

The strain amplitudes extracted from Locations 9 through 12 were used to determine the curvature ϕ for Section 1 using Equation 4. Then, the moment of inertia was computed using Equation 5 for each time window. Figure 16 shows the composite moment of inertia of Section 1 plotted against the cycle number. The moment of inertia was almost constant with an average value of about 450 in.^{4}. Figure 17 shows a similar graph for Section 2 that was obtained using the strain amplitudes collected from Locations 13 through 16. The average moment of inertia of this section was about 500 in.^{4} and was higher than that of Section 1. However, the moment of inertia for Section 2 was also almost constant.

Relative Displacement Between Deck and Beams

The amplitudes of the relative deck-beam displacements measured at Locations 1 through 5 were normalized with respect to the amplitude of the load. Figure 18 shows the normalized displacement amplitudes measured at Location 2 corresponding to the high-shear side of the north beam. The scattering of the points can be noted, but all values remained negligible,

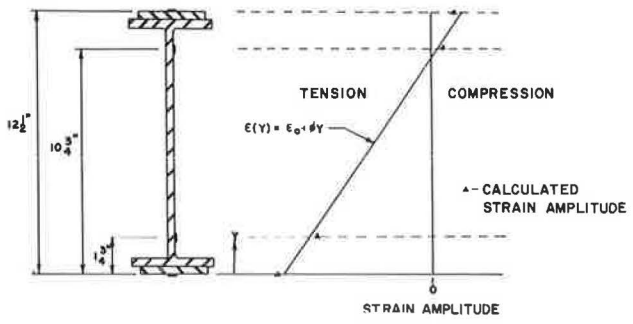

FIGURE 15 Straight-line fit of strain amplitudes at a section.

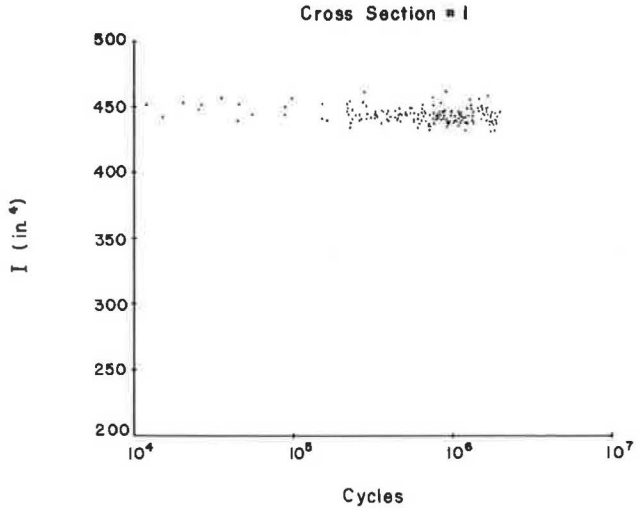

FIGURE 16 Dynamic composite moment of inertia of Section 1.

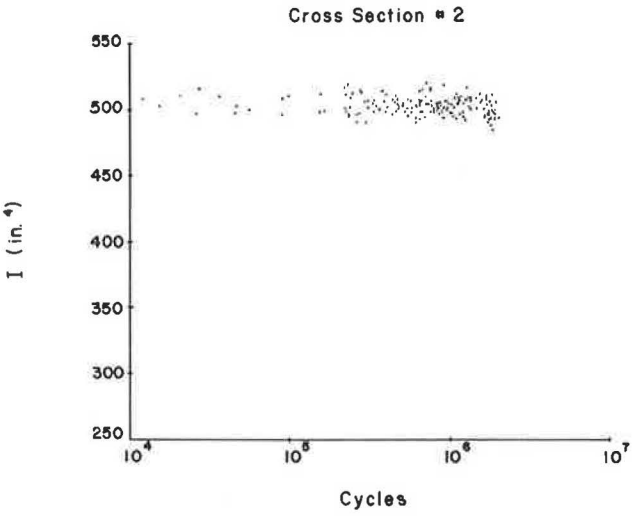

FIGURE 17 Dynamic composite moment of inertia of Section 2.

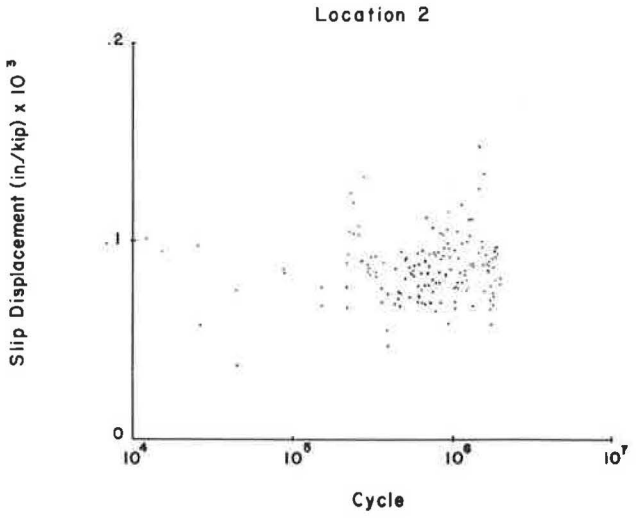

FIGURE 18 Relative normalized deck-beam horizontal displacement at Location 2.

so fracture or debonding of the interface connection between the deck and the beams was insignificant.

STATISTICAL SIGNIFICANCE OF TEST RESULTS

A statistical test was performed on the results to search for evidence of any deterioration of the bridge model during the load test. The statistical analysis was performed for the flexibilities at the quarter-points, the composite moments of inertia at Sections 1 and 2, and the relative displacements measured at the high-shear ends of the model (Locations 1 and 2). The following statistical assumptions were made:

- The relationships between the parameters involved and the logarithm of the cycle number were linear,
- The errors were statistically independent,
- The variance of the measurements was constant for each parameter, and
- The parameters were assumed normally distributed with means lying on a straight line.

The following procedure was adopted for this statistical test:

1. The flexibilities, the moments of inertia, and the relative displacement were assumed to be linear functions of the cycle number N, according to the expression

$$f(N) = \beta_0 + \beta_1 \log (N) \tag{6}$$

where

$f(N)$ = parameter function,
β_0 = intercept when $N = 1$, and
β_1 = slope of the regression equation.

2. After obtaining the linear regression coefficients, inferences about changes in the parameters were made by testing the null hypothesis (that the slope is zero) and its alternate hypothesis:

$$H_0: \beta_1 = 0 \tag{7}$$

$$H_a: |\beta_1| > 0 \tag{8}$$

When the null hypothesis is true, there is no statistical evidence of changes in the corresponding parameters. Alternately, H_a means that if the null hypothesis is not true, there is statistical evidence that the parameters changed.

3. The statistical test was made using the Student t-distribution, and the formula for the standard deviation of the slope β_1 was taken as

$$\sigma^2 = \left\{ \frac{\Sigma [f(N_i) - \beta_0 - \beta_1 \log N_i]^2}{n - 2} \right\} \tag{9}$$

4. An arbitrary probabilistic criterion was established to reject or accept the null hypothesis. The null hypothesis was rejected if there was a 90 percent probability that the magnitude of β_1 was greater than zero.

This statistical test was conducted on the data shown in Figures 11, 12–14, and 16–18, and also on the relative displacements at the high-shear ends of the beam (Locations 1 and 2). The results of the linear regression parameters and the probabilities that the slopes are not zero are presented in Tables 2–4.

Table 2 presents the results of the statistical test conducted on the flexibilities (Figures 12–14) obtained by measuring the deflections at the quarter-points of the north beam. From the

TABLE 2 STATISTICAL ANALYSIS RESULTS OF DYNAMIC FLEXIBILITIES

Location	β_0 (in./kip)	β_1 (in./kip)	$P[\lvert\beta_1\rvert>0]$
6, High Shear Side	0.0126	0.00020	0.99
7, Midspan	0.0156	0.00038	1.00
8, Low Shear Side	0.0113	0.00039	1.00

TABLE 3 STATISTICAL ANALYSIS OF COMPOSITE MOMENTS OF INERTIA

Section	β_0 (in^4)	β_1 (in^4)	$P[\lvert\beta_1\rvert>0]$
1	451.99	-1.589	0.98
2	506.99	-0.709	0.63

TABLE 4 STATISTICAL ANALYSIS OF RELATIVE DECK DISPLACEMENT

Location	β_0 (in./kip)	β_1 (in./kip)	$P[\lvert\beta_1\rvert>0]$
1, South Beam	$8.8X10^{-5}$	$8.6X10^{-6}$	0.85
2, North Beam	$6.4X10^{-5}$	$3.8x10^{-6}$	0.75

last column of this table, it is observed that the values are near (or equal to) 1.0. Therefore, there is enough statistical evidence that the flexibilities increased during the 2 million cycles of load. If the flexibilities at cycle 10,000 are taken as initial values, their percent increases after 2 million cycles were less than 7 percent. However, because no physical deteriorations were observed on the model or at the interface connections, the causes of these changes could not be inferred.

Table 3 presents the results of the statistical tests for the composite moments of inertia of Sections 1 and 2 (Figures 16 and 17). The properties of Section 1 deteriorated but there was no evidence of deteriorations of Section 2. The total percent decrease of the moment of inertia of Section 1 during the test was about 2 percent.

Table 4 presents the statistics results of the relative displacement measurements at the high-shear side of the bridge model. The table indicates that there is no convincing evidence that the relative displacements increased.

SUMMARY AND CONCLUSION

Two million sinusoidal cycles of an equivalent HS 20-44 AASHTO truck load were applied to a scaled laboratory model of a composite precast decked simple span bridge. Loads, deflections, strains, and relative displacements between the precast deck and the beams were measured at 826 time windows during the test. The measurements within each window were curve-fitted with a 3.5-Hz sinusoidal wave function from which the amplitudes of the measurements were determined. The amplitudes of deflections and relative deck-beam displacements were normalized and graphed against the number of cycles. From the strain amplitudes, the composite moment of inertia of two sections was obtained and graphed against the number of cycles. A statistical test was then conducted to establish the significance of the test results.

The following conclusions can be stated:

- The epoxy mortar and steel stud connection resisting the horizontal shear between the precast deck and the steel beams did not show signs of deteriorations after 2 million cycles of applied load. This conclusion was also justified by the lack of statistical evidence that the amplitudes of relative deck-beam displacements increased.
- The composite integrity of two instrumented cross sections of the bridge model was maintained throughout the applied loads. The composite moments of inertia decreased by less than 2 percent.
- The amplitudes of the measured deflections increased with increasing number of cycles, but the total increase from 10,000 to 2 million cycles was less than 7 percent. This increase could not be attributed to deteriorations of the interface connections.

With respect to design, it was clear after this experiment that to fatigue the shear connectors, the bonding action of the deck-beam interface material must fail first. The number of load cycles and the load levels applied to the model, which exceeded equivalent HS 20-44 load levels, were not sufficient to cause any fracture or debonding failure in the deck-beam interface epoxy material. Therefore, the presence of a good bond between the deck and the beams is extremely beneficial because the bond action prolongs the fatigue life of the shear connectors. To obtain a good bond, it is always recommended to follow placement and mixing instructions supplied by the epoxy manufacturer as well as to clean the bonding surfaces.

ACKNOWLEDGMENTS

This study was executed by the Texas Transportation Institute, The Texas A&M University System, and sponsored by the Texas State Department of Highways and Public Transportation in cooperation with FHWA, U.S. Department of Transportation.

REFERENCES

1. M. Biswas, J. S. B. Iffland, R. E. Schofield, and A. E. Gregory. Bridge Replacements with Precast Concrete Panels. *Special Report 148: Precast Bridge Deck Replacement Applications*, TRB, National Research Council, Washington, D.C., 1974, pp. 136–148.
2. C. V. Knudsen. Re-decking of a Bridge with Precast Concrete. *ASCE Civil Engineering*, Vol. 50, April 1980, pp. 75–77.
3. C. Slavis. Precast Concrete Deck Modules for Bridge Deck Reconstruction. In *Transportation Research Record 871*, TRB, National Research Council, Washington, D.C., 1982, pp. 30–32.
4. R. H. Berger. Full-Depth Modular Precast, Prestressed Bridge Decks. In *Transportation Research Record 903*, TRB, National Research Council, Washington, D.C., 1983, pp. 52–59.
5. J. G. Lutz and D. J. Scalia. Deck Widening and Replacement of Woodrow Wilson Memorial Bridge. *Journal of Prestressed Concrete Institute*, Vol. 29, No. 3, 1984, pp. 74–93.
6. M. M. Sprinkel. *NCHRP Synthesis of Highway Practice 119: Prefabricated Bridge Elements and Systems*. TRB, National Research Council, Washington, D.C., Aug. 1985, pp. 6–12.
7. *Standard Specifications for Highway Bridges*. AASHTO, Washington, D.C., 1983.

8. D. C. King, R. G. Slutter, and G. C. Driscoll. Fatigue Strength of ½-Inch Diameter Stud Shear Connectors. In *Highway Research Record 103*, HRB, National Research Council, Washington, D.C., 1965, pp. 78–106.
9. A. A. Toprac. Fatigue of ¾-Inch Stud Shear Connectors. In *Highway Research Record 103*, HRB, National Research Council, Washington, D.C., 1965, pp. 53–77.
10. R. G. Slutter and J. W. Fisher. Fatigue Strength of Shear Connectors. In *Highway Research Record 147*. HRB, National Research Council, Washington, D.C., 1966, pp. 58–65.
11. R. A. Osegueda and J. S. Noel. *Positive Moment Tests for Precast Concrete Panel-Decked Composite Bridges*. Research Report 324-1, Texas Transportation Institute, The Texas A&M University System, College Station, Sept. 1987.
12. F. E. Bonilla, R. W. James, R. A. Osegueda, and J. S. Noel. *Composite Action of Precast Panel Bridge Decks in Negative Moment Regions*. Research Report 324-2, Texas Transportation Institute, The Texas A&M University System, College Station, Sept. 1987.

Publication of this paper sponsored by Committee on Structures Maintenance.